Many-body quantum non-Markovianity

Jonathan Brugger[1,2] Christoph Dittel[1,2,3] and Andreas Buchleitner[1,2]
[1]*Physikalisches Institut, Albert-Ludwigs-Universität Freiburg, Hermann-Herder-Straße 3, 79104 Freiburg, Germany*
[2]*EUCOR Centre for Quantum Science and Quantum Computing, Albert-Ludwigs-Universität Freiburg, Hermann-Herder-Straße 3, 79104 Freiburg, Germany*
[3]*Freiburg Institute for Advanced Studies, Albert-Ludwigs-Universität Freiburg, Albertstraße 19, 79104 Freiburg, Germany*

(Received 19 August 2022; revised 8 December 2022; accepted 16 March 2023; published 26 April 2023)

We port the concept of non-Markovian quantum dynamics to the many-particle realm, by a suitable decomposition of the many-particle Hilbert space. We show how the specific structure of many-particle states determines the observability of non-Markovianity by single- or many-particle observables, and discuss a realization in a readily implementable few-particle setup.

DOI: 10.1103/PhysRevResearch.5.023060

I. INTRODUCTION

Non-Markovian behavior [1] is the partial restoration of an open quantum system's memory of its past. In general, we expect that an open quantum system – widely (though not exclusively) understood as living on a small number of degrees of freedom, as opposed to the many degrees of freedom of an environment or bath it is coupled to – tends to irreversibly lose its memory since any information leaking to the environment will quickly disperse and not relocalize on the system degrees of freedom [2–4]. However, this intuition is reliable only if the number of degrees of freedom associated with system and environment, as well as the associated spectral structures, are distinct, and when system and environment do not easily correlate. Consequently, non-Markovian behavior is naturally expected, e.g., in large molecular structures [5–9], where different degrees of freedom are strongly coupled and typically nonseparable, with the consequence that Markovian master equationlike descriptions (successfully employed for many quantum optical applications [2]) become unreliable. Given the ever-improving experimental resolution of the dynamics of diverse multicomponent quantum systems [10–15], there is a strong incentive to improve our understanding of non-Markovianity and to identify observables which allow for an unambiguous identification of non-Markovian effects.

While the prerequisites for Markovian behavior have been long known [2,3], the concept of non-Markovianity needed to be formalized, and many of its subtleties have been clarified [1,16–22] in recent years. Yet, the specific impact of the generic structural features of many-particle systems upon the manifestations of non-Markovianity hitherto have remained unexplored. Our present contribution specifically addresses non-Markovianity in the many-particle context.

II. NON-MARKOVIANITY ON A MANY-PARTICLE HILBERT SPACE

We rely on the definition and quantification of non-Markovian behavior in terms of information backflow from the environment into the system, through the time dependence of the trace distance [1,17],

$$D(\rho,\sigma) = \tfrac{1}{2}\mathrm{tr}|\rho-\sigma|, \tag{1}$$

of initially distinct system states ρ and σ, with $|M| = \sqrt{MM^\dagger}$ the positive square root of a positive semidefinite operator. D is a metric on the space of density matrices, with $D(\rho,\sigma) = 0$ if and only if $\rho = \sigma$, and $D(\rho,\sigma) = 1$ if and only if ρ and σ have orthogonal support [1]. As an exhaustive measure for the distinguishability of two quantum states – by any type of measurement – it quantifies their distinctive information content. Consequently, any increase of the trace distance $D(\rho,\sigma)$ over time, tantamount to restoring the information on the system states' initial distinguishability, indicates non-Markovianity. However, when state tomography turns unaffordable, e.g., due to the underlying Hilbert space dimension [23], it is *a priori* often unclear which observable can expose such distinctive information most efficiently, and particularly so when dealing with many-particle states.

A. The structure of many-particle state space

As we show in the following, such observables can be found through examination of the intriguing, nontrivial structure of the many-particle state space. To this end, we first consider the general problem of open many-particle quantum systems, before treating explicit examples: Let us assume that we are given a potential landscape which omits a natural decomposition of the total single-particle Hilbert space $\mathcal{H}$ into two distinct subspaces, associated with the principal system (S) and environment (E), via a direct sum, $\mathcal{H} = \mathcal{H}_\mathrm{S} \oplus \mathcal{H}_\mathrm{E}$, with $\mathcal{H}_\mathrm{S}$ and $\mathcal{H}_\mathrm{E}$ the state spaces of the system and the environment, respectively. Any pure state of the system and environment can then be written as $|\psi\rangle = \Pi_\mathrm{S}|\psi\rangle + \Pi_\mathrm{E}|\psi\rangle$,

with $\Pi_{S(E)}$ the projector onto $\mathcal{H}_{S(E)}$, and $P_1 = \langle\psi|\Pi_S|\psi\rangle$ the probability to find the particle in the system. The many-particle dynamics of $N \geqslant 1$ identical bosons (fermions) in that potential landscape play in the Fock space $\Gamma^{b(f)}(\mathcal{H})$ [24], which can be constructed from the single-particle Hilbert space $\mathcal{H} = \mathcal{H}_S \oplus \mathcal{H}_E$ and factorized [25,26] as

$$\Gamma^{b(f)}(\mathcal{H}_S \oplus \mathcal{H}_E) \cong \Gamma^{b(f)}(\mathcal{H}_S) \otimes \Gamma^{b(f)}(\mathcal{H}_E). \tag{2}$$

This *tensor product* structure enables the interpretation as an open quantum system, despite the *direct sum* structure of $\mathcal{H}$ (rather reminiscent of an atomic ionization problem [27]).

For a pure N-particle state with initial support on the system degrees of freedom alone (i.e., all N particles in the system and none in the environment), unitary dynamics and a well-defined particle number on the combined system and environment degrees of freedom restrict the time evolution to the effective N-particle space

$$\mathcal{H}_{\text{eff}}^N = \bigoplus_{k=0}^{N} \left(\mathcal{H}_S^{\otimes k} \otimes \mathcal{H}_E^{\otimes(N-k)}\right)_{s(a)} \subsetneq \Gamma^{b(f)}(\mathcal{H}), \tag{3}$$

with the (anti)symmetrization $\mathcal{X}_{s(a)}$ of a Hilbert space $\mathcal{X}$. As a consequence, every pure state of system and environment can be written as $|\psi\rangle = \sum_{k=0}^{N} c_k\,|\psi_k\rangle \in \mathcal{H}_{\text{eff}}^N$, with real, non-negative amplitudes c_k, and $|\psi_k\rangle$ a state with k out of N particles confined to the system [28].

B. Many-particle non-Markovianity quantifiers and bounds

To assess the non-Markovian character of the system dynamics, we need to trace $|\psi\rangle\langle\psi|$ over the environment, to produce the reduced system state

$$\rho_S = \text{tr}_E|\psi\rangle\langle\psi| = \sum_{k=0}^{N} c_k^2\,\rho_k, \tag{4}$$

with $\rho_k = \text{tr}_E|\psi_k\rangle\langle\psi_k|$. The partial trace tr_E is natural for the tensor product in Eq. (2), and well-defined for $|\psi\rangle\langle\psi|$ by restriction to $\mathcal{H}_{\text{eff}}^N$. Intuitively, it can be thought of as tracing over the $N-k$ particles in the environment for each summand in Eq. (3). The reduced state ρ_S exhibits a block-diagonal structure since the total particle number N is conserved and states of the environment corresponding to different particle numbers are orthogonal. The trace distance $D(\rho_S, \sigma_S)$ between two reduced states $\rho_S = \sum_k c_k^2\rho_k$ and $\sigma_S = \sum_k d_k^2\sigma_k$ of the system can now be evaluated for arbitrary particle number, particle type (bosons or fermions), degree of (in)distinguishability, and interaction strength and type, as

$$D(\rho_S, \sigma_S) = \sum_{k=0}^{N} D\big(c_k^2\rho_k, d_k^2\sigma_k\big). \tag{5}$$

Whenever $D(\rho_S, \sigma_S)$ increases as a function of time, it signals non-Markovian behavior. Although the block-diagonal structure of ρ_S and σ_S significantly reduces the computational complexity of the trace distance $D(\rho_S, \sigma_S)$, it remains nontrivial to evaluate, especially for the dynamics of many *interacting* particles. However, as we show in the following, this burden can often be alleviated by relating the trace distance $D(\rho_S, \sigma_S)$ to computationally and experimentally more readily accessible quantities.

From Eq. (4), we obtain the probabilities $P_k(\rho_S) = c_k^2$ to find *exactly* k out of N particles in the system, which constitute simple many-particle observables (given the availability of number-resolving detectors) and are useful to distinguish Markovian from non-Markovian many-body dynamics. As we show in the Appendix, these probabilities allow us to bound the trace distance by

$$P_{\text{est}}^{\ell} \leqslant D(\rho_S, \sigma_S) \leqslant P_{\text{est}}^{\text{u}}, \tag{6}$$

with the lower and upper bounds given by

$$P_{\text{est}}^{\ell} = \sum_{k=0}^{N} \frac{\left|c_k^2 - d_k^2\right|}{2} \tag{7}$$

and

$$P_{\text{est}}^{\text{u}} = 1 - \frac{c_0^2 + d_0^2}{2} + \frac{\left|c_0^2 - d_0^2\right|}{2}, \tag{8}$$

respectively. Intuitively, P_{est}^{ℓ} is the sum of *minimal* trace distances within the blocks in (4), each given by the associated population differences. Analogously, $P_{\text{est}}^{\text{u}}$ is the sum of the *exact* trace distance in the one-dimensional block $k = 0$, and of the *maximal* trace distances within all blocks $k \geqslant 1$, again given by population differences.

Similarly, we can bound the trace distance $D(\rho_S, \sigma_S)$ in terms of single-particle observables. To this end, we consider the *reduced single-particle density matrix* (RSPDM),

$$\rho_S^{1p} = \text{tr}_{2,\ldots,N}\rho_S = c_0^2\,\rho_0 + c_1^2\,\rho_1 + \sum_{k=2}^{N} c_k^2\,\text{tr}_{2,\ldots,k}\rho_k, \tag{9}$$

obtained from the system's state (4) by tracing out all but one particle [29,30]. It describes a potentially mixed state with up to one particle in the system and offers a natural way to compare states on a single-particle level since the expectation value (with respect to ρ_S) of any single-particle observable (such as, e.g., the projection $|1\rangle\langle 1|$ onto the single-particle ground state) can be inferred from it [30]. Using the contractivity of D under trace-preserving quantum operations [31,32], we find

$$D\big(\rho_S^{1p}, \sigma_S^{1p}\big) \leqslant D(\rho_S, \sigma_S), \tag{10}$$

again bounding the trace distance from below.

While an *exact quantification* of non-Markovianity involves a maximization of the increase in trace distance over different pairs of initial states [1], our bounds (6)–(10) on $D(\rho_S, \sigma_S)$ allow for the direct *certification* of non-Markovianity in the system dynamics (providing a lower bound rather than a quantifier) by monitoring simple features of the counting statistics or of single-particle observables such as the ground state population of the system as a function of time. Explicitly, any two points in time $t_0 < t_1$ for which either $P_{\text{est}}^{\text{u}}(t_0) < P_{\text{est}}^{\ell}(t_1)$ or $P_{\text{est}}^{\text{u}}(t_0) < D[\rho_S^{1p}(t_1), \sigma_S^{1p}(t_1)]$ imply a temporally increasing trace distance $D(\rho_S, \sigma_S)$ and therefore – by definition – non-Markovian behavior. This ultimately connects the information flow between system and environment in many-particle quantum systems to the structure of many-body state space, through the populations P_k of different k-particle blocks and the population distribution over reduced single-particle states as given by the RSPDM.

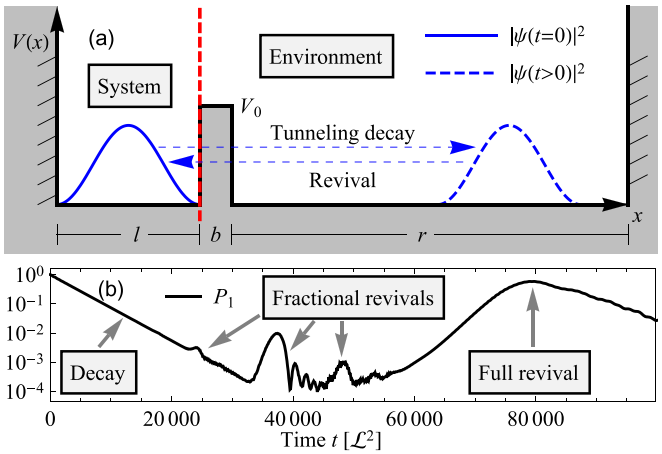

FIG. 1. Tunneling in a one-dimensional asymmetric double-well potential. (a) Sketch: A particle prepared [continuous blue line, $|\psi(t=0)|^2$] in the left well (system) tunnels into the right well (environment), is reflected at the right boundary, and possibly reenters the system [dashed blue line, $|\psi(t>0)|^2$]. (b) Semilogarithmic plot of the particle's probability P_1 to be found in the system, if initially prepared in the isolated system's ground state $|1\rangle$, for $l = 50\,\mathcal{L}$, $b = 2\,\mathcal{L}$, $r = 4000\,\mathcal{L}$, and $V_0 = 0.1\,\mathcal{L}^{-2}$.

III. AN EXEMPLARY TEST CASE: MANY-PARTICLE DYNAMICS IN AN ASYMMETRIC DOUBLE-WELL

Intuitively, information flow is associated with the exchange of excitations in different degrees of freedom. In the following, we build on this intuition by considering the specific – and experimentally feasible [33] – example of few fermions or bosons loaded into the asymmetric, one-dimensional double-well potential depicted in Fig. 1(a): Left and right potential wells of width l and r each define local mode structures which we associate with the system's and environmental degrees of freedom, respectively. They are separated by a finite rectangular barrier of width b and height V_0, which is part of the environment. As shown earlier [34–36], this model allows an exact spectral treatment of the decay dynamics of an open many-body system with a continuously tunable, discrete to quasicontinuous spectral structure of the environment. System-environment coupling is determined by b and V_0, and weak coupling and a quasicontinuous spectrum of the environment, in the limit of large r, justify the intuition of the system being opened to couple to the environment's degree of freedom.

A. Detecting non-Markovianity of single-particle dynamics

Single-particle dynamics are obtained from exact numerical diagonalization [37] of the single-particle Hamiltonian $H_{\rm sp}(x) = -\partial^2/\partial x^2 + V(x)$, after discretization in a suitable finite-element basis [38,39]. While we will elaborate elsewhere [37] on how to control the arising non-Markovian tunneling dynamics by tuning, through variable r, the transition to a quasicontinuum, we here focus on a fixed, finite width r, which generates the typical behavior. In all subsequent simulations, we choose the parameters $l = 50\,\mathcal{L}$, $b = 2\,\mathcal{L}$, $r = 4000\,\mathcal{L}$, and $V_0 = 0.1\,\mathcal{L}^{-2}$, given in natural units, with $\hbar \equiv 1$ and mass $m \equiv 1/2$, and in terms of the characteristic experimental length scale $\mathcal{L}$ [35]. These values, in particular, establish the quasicontinuous limit for the environment's spectrum, notwithstanding the hard-wall boundary condition of the right well's outer confinement, which clearly induces non-Markovian behavior on sufficiently long timescales [35,36].

While all stated conceptual observations and analytical results apply, in particular, also for interacting particles, we restrict our subsequent numerical examples to the non-interacting case, such that many-particle eigenstates are (anti)symmetrized product states of single-particle eigenstates (interacting particles will be considered elsewhere [37]). To consider distinguishable, indistinguishable, and partially distinguishable particles [40], we further equip the particles with an internal degree of freedom, e.g., $\mathcal{H}_{\rm int} = {\rm span}\{|+\rangle, |-\rangle\}$, unobservable by any available measurement and not coupled to their external degree of freedom [i.e., $H_{\rm sp}(x)$ is independent of the particle's internal state]. The tightness of the bounds (6)–(10) is inspected for different instructive examples of initial single- and many-particle states ρ and σ, with the results shown in Figs. 2 and 3, respectively. In all examples, there are initially no particles located in the environment, such that the initial states are separable, $\rho(0) = \rho_{\rm S}(0) \otimes |0_{\rm E}\rangle\langle 0_{\rm E}|$ and $\sigma(0) = \sigma_{\rm S}(0) \otimes |0_{\rm E}\rangle\langle 0_{\rm E}|$, with $\rho_{\rm S}(0)$ and $\sigma_{\rm S}(0)$ many-body eigenstates of the left well, and $|0_{\rm E}\rangle$ the vacuum state of the environment.

Starting with single-particle dynamics, Fig. 1(b) shows the time evolution of the probability $P_1 = \langle\psi|\Pi_{\rm S}|\psi\rangle = c_1^2$ for the particle to be detected in the left well after being initialized in the ground state $|1\rangle$ of the isolated system. We observe an exponential decay, followed by low-amplitude (note the semilogarithmic scale) partial (fractional) [41] revivals, and, subsequently, a pronounced full revival. Fractional and full revivals are due to the coherent superposition of single-particle amplitudes reflected at the barrier and at the right boundary of the environment, with an admixture of nonvanishing excited state amplitudes of the system degree of freedom. The latter define the fractional revival times in Fig. 1(b) and are individually enhanced when launching the dynamics in an excited system state, as, e.g., $|2\rangle$ in Fig. 2(a). Since such revivals express excitation and, thus, information backflow into the system degree of freedom, they are indicative of non-Markovianity.

Figures 2(a) and 2(b) compare the evolution of the auto- and cross correlation functions of two pure single-particle states, launched in the system's ground and first excited states, respectively, upon trace over the environment according to (4), to the time evolution of the trace distance (5). We see that the revival dynamics of the system state populations in Fig. 2(a) is faithfully reflected by the trace distance in Fig. 2(b), and almost everywhere reproduced by the lower bound $P^{\ell}_{\rm est}$, thus comforting our intuition that information backflow is synonymous to excitation backflow. However, we also see from the mismatch between $P^{\ell}_{\rm est}$ and $D(\rho_{\rm S}, \sigma_{\rm S})$ at $t \approx 74\,000\,\mathcal{L}^2$, where both autocorrelation functions revive simultaneously, that $P^{\ell}_{\rm est}$, which only monitors the population difference in the system, without resolving individual system state populations, is then too coarse grained a quantifier to distinguish both states. Likewise, the reviving trace distance of two pure single-particle states both launched in the system's

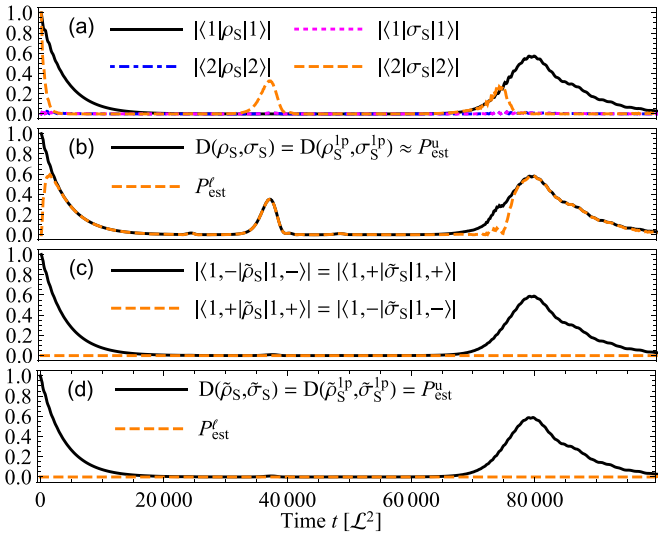

FIG. 2. Non-Markovian single-particle tunneling in an asymmetric double-well potential (see Fig. 1). (a) The autocorrelation functions $|\langle 1|\rho_S|1\rangle|$ and $|\langle 2|\sigma_S|2\rangle|$ of a single particle initially prepared in the ground state $|1\rangle$ or in the first excited state $|2\rangle$, respectively, of the isolated left potential well and reduced to the system, i.e., to the left well's degrees of freedom, show clear revivals after their initial exponential decay, with a shorter revival time for the first excited state $|2\rangle$ in comparison to the ground state $|1\rangle$. The cross correlation functions $|\langle 2|\rho_S|2\rangle|$ and $|\langle 1|\sigma_S|1\rangle|$ exhibit no such revivals. (b) The revivals in (a) are faithfully reflected by the trace distance $D(\rho_S, \sigma_S)$, given by Eq. (5), as well as, almost everywhere, by its estimators (7), (8), and (10) [$P_{est}^{u} \approx D(\rho_S, \sigma_S)$, with deviations smaller than 10^{-2}]. Only at $t \approx 74\,000\,\mathcal{L}^2$ is the lower bound P_{est}^{ℓ}, given by Eq. (7), not tight, since it does not resolve single state population differences, but only those of the total particle number probabilities in the left well. For the same reason, P_{est}^{ℓ} is unable to discriminate single-particle states launched in the ground state $|1\rangle$, but labeled with mutually orthogonal states $|\pm\rangle$ in an additional degree of freedom: (d) Only the estimators (8) and (10) and the trace distance $D(\tilde{\rho}_S, \tilde{\sigma}_S)$ sense the revivals featured by (c) the autocorrelation functions $|\langle 1, -|\tilde{\rho}_S|1, -\rangle|$ and $|\langle 1, +|\tilde{\sigma}_S|1, +\rangle|$.

ground state, but labeled by mutually orthogonal states of an additional degree of freedom, is faithfully reproduced by P_{est}^{u} and $D(\rho_S^{1p}, \sigma_S^{1p})$, while P_{est}^{ℓ} is blind for this distinction, by its very construction. The latter is in contrast to the estimate P_{est}^{u}, which is tight in Fig. 2(d), as the particles are prepared in and return to orthogonal single-particle modes of the system, thus realizing the maximal trace distance assumed in the derivation of (8). Similarly, in Fig. 2(b), the particles return into essentially orthogonal states and approximately realize the aforementioned maximum.

B. Detecting non-Markovianity of many-particle dynamics

On the many-particle level, a nonvanishing trace distance can have different physical causes, including – in our present case of noninteracting particles – different constituting single-particle states, particle numbers, and symmetry properties. Let us inspect how to sense such differences using the bounds derived above. Figure 3(a) monitors the trace distance $D(\rho_S, |0_S\rangle\langle 0_S|)$ of the reduced system state of three

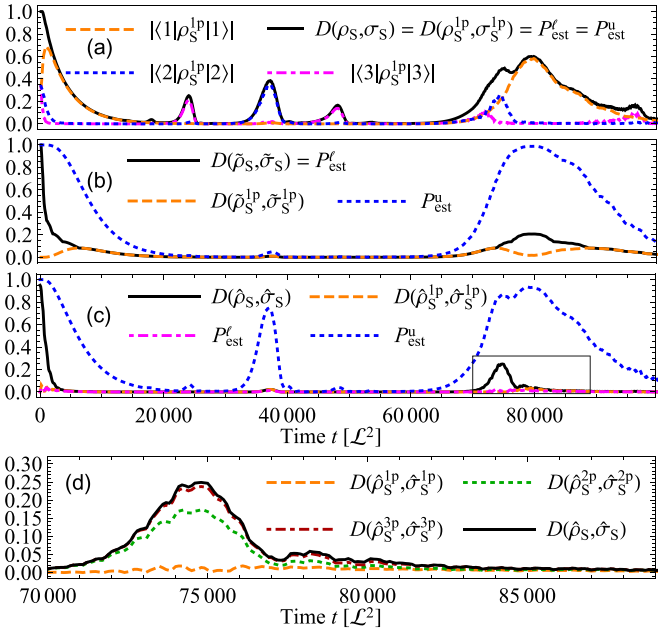

FIG. 3. Non-Markovian many-particle tunneling: (a) Three indistinguishable fermions launched in the (fermionic) ground state of the isolated left well (see Fig. 1), with no particles initially in the right well, exhibit clear revivals of the reduced single-particle autocorrelation functions $|\langle j|\rho_S^{1p}|j\rangle|$, $j = 1, 2, 3$, of the left well's ground, first, and second excited single-particle states. This gives rise to non-Markovian behavior as clearly manifest in the state's trace distance $D(\rho_S, \sigma_S)$ from the left well's (time-invariant) many-particle vacuum state $\sigma_S = |0_S\rangle\langle 0_S|$. The trace distance estimators $D(\rho_S^{1p}, \sigma_S^{1p})$, P_{est}^{ℓ}, P_{est}^{u}, (7), (8), and (10), are tight, since $d_k = \delta_{0k}$ for the many-particle vacuum state. (b) and (c) monitor the trace distance and its estimators (7), (8), and (10) for two pairs of bosonic many-particle states, again with all particles launched in a many-particle eigenstate of the isolated left well: The trace distance $D(\tilde{\rho}_S^{1p}, \tilde{\sigma}_S^{1p})$ of the reduced single-particle states of the four- and five-particle states launched in the bosonic ground states (b) of the isolated left well, $\tilde{\rho}(0) = \tilde{\rho}_S(0) = |1\rangle\langle 1|^{\otimes 4}$ and $\tilde{\sigma}(0) = \tilde{\sigma}_S(0) = |1\rangle\langle 1|^{\otimes 5}$, respectively, only barely detects the many-body revival in the system ground state. To detect non-Markovianity by comparison of (c) the many-particle dynamics of six particles prepared in $\hat{\rho}(0) = \hat{\rho}_S(0) = \mathcal{S}(|1\rangle\langle 1|^{\otimes 3} \otimes |2\rangle\langle 2|^{\otimes 3})$ and $\hat{\sigma}(0) = \hat{\sigma}_S(0) = |1\rangle\langle 1|^{\otimes 3} \otimes |2\rangle\langle 2|^{\otimes 3}$, respectively, which differ only by their (un)symmetrized character ($\mathcal{S}$ is the bosonic symmetrization operator), bona fide many-particle observables need to be interrogated. The latter is verified in (d), the magnification of the prominent revival of the trace distance indicated by the black rectangle in (c), through the trace distance estimators $D(\hat{\rho}_S^{kp}, \hat{\sigma}_S^{kp})$ for $1 \leqslant k \leqslant 3$ [not shown are $D(\hat{\rho}_S^{kp}, \hat{\sigma}_S^{kp}) \approx D(\hat{\rho}_S, \hat{\sigma})$ for $k \geqslant 4$], which faithfully indicate the trace distance revival for $k \geqslant 2$.

noninteracting, indistinguishable fermions, launched in the system ground state, from the (time-invariant) many-particle system vacuum $|0_S\rangle$, as well as the trace distance estimates (7), (8), and (10), which here all coincide with the full trace distance [37]. The three fermions initially populate the system's single-particle eigenstates $|1\rangle$, $|2\rangle$, and $|3\rangle$, and undergo – up to the antisymmetrization – their individual single-particle dynamics, as depicted in Fig. 2 for $|1\rangle$ and $|2\rangle$. The resulting recombinations of the individual particles into

the ground, first, and second excited system state, as clearly reflected by the revivals of the reduced state single-particle autocorrelation functions $|\langle j|\rho_{\mathrm{S}}^{1\mathrm{p}}|j\rangle|$, induce non-Markovianity of the three-particle state's dynamics, as unambiguously indicated by synchronous revivals of the above distance measures.

Figure 3(b) shows the time evolution of the trace distance of bosonic four- and five-particle states launched in the system ground states, $\tilde{\rho}(0) = \tilde{\rho}_{\mathrm{S}}(0) = |1\rangle\langle 1|^{\otimes 4}$ and $\tilde{\sigma}(0) = \tilde{\sigma}_{\mathrm{S}}(0) = |1\rangle\langle 1|^{\otimes 5}$, respectively. Here, non-Markovianity stems from a many-particle repopulation of the system single-particle ground state, which, due to dispersion within the environment, stretches over a longer time interval, thus leading to an only mild revival of the states' trace distance. The reduced single-particle states are barely discriminated by the single-particle trace distance, on the rising and on the falling edge of the repopulation of the system ground state, and cannot be distinguished at the maximum of the many-particle revival (by construction). Figures 2(b) and 3(b) therefore demonstrate that the lower bounds (6) and (10) are complementary: non-Markovianity arising from different particle numbers is best detected by P_{est}^{ℓ}, whereas $D(\rho_{\mathrm{S}}^{1\mathrm{p}}, \sigma_{\mathrm{S}}^{1\mathrm{p}})$ is sensitive to the population of different single-particle states.

While the bosonic many-particle states in Fig. 3(b) are distinguished by their particle numbers, Fig. 3(c) considers two $(N = 6)$-particle states of identical bosons [40], with identical and pairwise orthogonal internal states, respectively. Recall that the internal states are unobservable by any available measurement and are therefore traced over, resulting in many-body states of indistinguishable and effectively distinguishable bosons, respectively. However, these differences in the states' symmetry properties are irrelevant if all particles located in the left well populate the same single-particle state. Consequently, the resulting many-body states $\hat{\rho}_{\mathrm{S}}$ and $\hat{\sigma}_{\mathrm{S}}$ of the reduced system only differ if at least two particles in different single-particle states populate the system at the same time. We therefore specifically consider $\hat{\rho}(0) = \hat{\rho}_{\mathrm{S}}(0) = \mathcal{S}(|1\rangle\langle 1|^{\otimes 3} \otimes |2\rangle\langle 2|^{\otimes 3})$ and $\hat{\sigma}(0) = \hat{\sigma}_{\mathrm{S}}(0) = |1\rangle\langle 1|^{\otimes 3} \otimes |2\rangle\langle 2|^{\otimes 3}$, with initially three particles in each, the ground and the first excited system state, respectively, and $\mathcal{S}$ the bosonic symmetrization operator. Both initial states can be told apart only from their symmetry properties, by (reduced) k-particle trace distances $D(\hat{\rho}_{\mathrm{S}}^{k\mathrm{p}}, \hat{\sigma}_{\mathrm{S}}^{k\mathrm{p}})$ with $N \geqslant k > 1$ [42] and neither from single-particle nor number state populations, underlining the inherent complexity of such many-body states. Consequently, none of the estimates (7), (8), or (10) provides a tight approximation of the time-evolved states' actual trace distance $D(\hat{\rho}_{\mathrm{S}}, \hat{\sigma}_{\mathrm{S}})$, which exhibits a weak revival at $t \approx 74\,000\,\mathcal{L}^2$ due to the partially overlapping return of particles into the system's ground and first excited state [see also Fig. 2(a)]. Only true many-body measurements can detect such a symmetry-induced trace distance revival, as demonstrated by the reduced k-particle trace distances $D(\hat{\rho}_{\mathrm{S}}^{k\mathrm{p}}, \hat{\sigma}_{\mathrm{S}}^{k\mathrm{p}})$ in Fig. 3(d). Finally, the results in Figs. 3(b) and 3(c) emphasize that $P_{\mathrm{est}}^{\mathrm{u}}$ – by construction – only guarantees a tight upper bound for $D(\rho_{\mathrm{S}}, \sigma_{\mathrm{S}})$ if either ρ_{S} or σ_{S} is sufficiently close to the many-particle vacuum.

IV. CONCLUSION

We thus have seen that the non-Markovianity of N-body open system quantum evolution may be certifiable through experimentally readily accessible single-particle observables such as state populations or occupation numbers – which can be inferred from the compared many-body states' reduced single-particle density matrices. Though, depending on the choice of reference states, such certification may also require to assess information inscribed into the latter's reduced $(k > 1)$-particle system states for a discrimination on the level of many-body correlations and/or of quantum statistical features. This hierarchical nesting of distinctive properties is resolved by the many-body version of the reference states' trace distance derived here – given as a sum over trace distances of k-particle states since the particle number is generally *not* conserved in an open many-body system. The decomposition into k-particle contributions, with $0 \leqslant k \leqslant N$, crucially relies on our identification of the relevant tensor structure of the many-body Fock space erected upon the single-particle Hilbert space (itself given as a direct sum), since it is this tensor structure which reveals a many-body state's open system dynamics.

ACKNOWLEDGMENTS

The authors thank Heinz-Peter Breuer and Moritz Richter for fruitful discussions. J.B. thanks the Studienstiftung des deutschen Volkes for support. C.D. acknowledges the Georg H. Endress foundation for financial support and the Freiburg Institute for Advanced Studies for a FRIAS Junior Fellowship.

APPENDIX: DERIVATION OF THE BOUNDS IN (6)

First, note that the normalization of the states ρ_{S} and σ_{S} implies

$$\sum_{k=0}^{N} c_k^2 = \sum_{k=0}^{N} d_k^2 = 1. \tag{A1}$$

Next, from the triangle inequality [32], it follows that

$$D\big(c_k^2\rho_k, d_k^2\sigma_k\big) \leqslant D\big(c_k^2\rho_k, 0\big) + D\big(0, d_k^2\sigma_k\big) = \frac{c_k^2 + d_k^2}{2}, \tag{A2}$$

with the zero operator 0 (the additive neutral element in the Banach space of trace class operators [43]), and from the reverse triangle inequality, we get

$$D\big(c_k^2\rho_k, d_k^2\sigma_k\big) \geqslant \big|D\big(c_k^2\rho_k, 0\big) - D\big(0, d_k^2\sigma_k\big)\big| = \frac{\big|c_k^2 - d_k^2\big|}{2}. \tag{A3}$$

Note that this also holds for non-normalized operators $c_k^2\rho_k$ and $d_k^2\sigma_k$ since the trace norm $\|A\|_1 = \mathrm{tr}|A|$ is a norm on the space of trace class operators [43], and its induced metric is – up to the prefactor $1/2$ – the trace distance. Finally, for the one-dimensional subspace with $k = 0$ particles in the system, we have $\rho_0 = \sigma_0 = |0_{\mathrm{S}}\rangle\langle 0_{\mathrm{S}}|$ and, thus,

$$D\big(c_0^2\rho_0, d_0^2\sigma_0\big) = \frac{\big|c_0^2 - d_0^2\big|}{2}. \tag{A4}$$

The upper bound in (6) then follows from (5), (A4), (A2), and (A1),

$$D(\rho_S,\sigma_S)=\sum_{k=0}^{N}D\big(c_k^2\rho_k,d_k^2\sigma_k\big)\leqslant\frac{|c_0^2-d_0^2|}{2}+\sum_{k=1}^{N}\frac{c_k^2+d_k^2}{2}$$
$$=1+\frac{|c_0^2-d_0^2|}{2}-\frac{c_0^2+d_0^2}{2},$$

while the lower bound directly follows from (5) and (A3),

$$D(\rho_S,\sigma_S)\geqslant\sum_{k=0}^{N}\frac{|c_k^2-d_k^2|}{2}.$$

[1] H.-P. Breuer, E.-M. Laine, J. Piilo, and B. Vacchini, Colloquium: Non-Markovian dynamics in open quantum systems, Rev. Mod. Phys. **88**, 021002 (2016).

[2] C. Cohen-Tannoudji, J. Dupont-Roc, and G. Grynberg, *Atom-Photon Interactions – Basic Processes and Applications* (Wiley-VCH Verlag, 2004).

[3] A. R. Kolovsky, Number of degrees of freedom for a thermostat, Phys. Rev. E **50**, 3569 (1994).

[4] A. Buchleitner and A. R. Kolovsky, Interaction-Induced Decoherence of Atomic Bloch Oscillations, Phys. Rev. Lett. **91**, 253002 (2003).

[5] P. Rebentrost, R. Chakrborty, and A. Aspuru-Guzik, Non-Markovian quantum jumps in excitonic energy transfer, J. Chem. Phys. **131**, 184102 (2009).

[6] M. Walschaers, Jorg Fernandez-de-Cossio Diaz, R. Mulet, and A. Buchleitner, Optimally Designed Quantum Transport Across Disordered Networks, Phys. Rev. Lett. **111**, 180601 (2013).

[7] H.-B. Chen, N. Lambert, Y.-C. Cheng, Y.-N. Chen, and F. Nori, Using non-Markovian measures to evaluate quantum master equations for photosynthesis, Sci. Rep. **5**, 12753 (2015).

[8] F. Levi, S. Mostarda, F. Rao, and F. Mintert, Quantum mechanics of excitation transport in photosynthetic complexes: A key issues review, Rep. Prog. Phys. **78**, 082001 (2015).

[9] J. J. Roden, D. I. G. Bennett, and K. B. Whaley, Long-range energy transport in photosystem II, J. Chem. Phys. **144**, 245101 (2016).

[10] C. A. Rozzi, S. M. Falke, N. Spallanzani, A. Rubio, E. Molinari, D. Frida, M. Maiuri, G. Cerullo, H. Schramm, J. Christoffers, and C. Lienau, Quantum coherence controls the charge separation in a prototypical artificial light-harvesting system, Nat. Commun. **4**, 1602 (2013).

[11] F. Meinert, M. J. Mark, E. Kirilov, K. Lauber, P. Weinmann, M. Gröbner, and H.-C. Nägerl, Interaction-Induced Quantum Phase Revivals and Evidence for the Transition to the Quantum Chaotic Regime in 1D Atomic Bloch Oscillations, Phys. Rev. Lett. **112**, 193003 (2014).

[12] P. Malý, J. M. Gruber, R. J. Cogdell, T. Mancal, and R. van Grondelle, Ultrafast energy relaxation in single light-harvesting complexes, Proc. Natl. Acad. Sci. USA **113**, 2934 (2016).

[13] M. Wittemer, G. Clos, H.-P. Breuer, U. Warring, and T. Schaetz, Measurements of quantum memory effects and its fundamental limitations, Phys. Rev. A **97**, 020102(R) (2018).

[14] L. Bruder, U. Bangert, M. Binz, D. Uhl, and F. Stienkemeier, Coherent multidimensional spectroscopy in the gas phase, J. Phys. B **52**, 183501 (2019).

[15] B. Wittmann, F. A. Wenzel, S. Wiesneth, A. T. Handler, M. Drechsler, K. Kreger, J. Köhler, E. W. Meijer, H.-W. Schmidt, and R. Hildner, Enhancing long-range energy transport in supramolecular architectures by tailoring coherence properties, J. Am. Chem. Soc. **142**, 8323 (2020).

[16] M. M. Wolf, J. Eisert, T. S. Cubitt, and J. I. Cirac, Assessing Non-Markovian Quantum Dynamics, Phys. Rev. Lett. **101**, 150402 (2008).

[17] H.-P. Breuer, E.-M. Laine, and J. Piilo, Measure for the Degree of Non-Markovian Behavior of Quantum Processes in Open Systems, Phys. Rev. Lett. **103**, 210401 (2009).

[18] A. Rivas, S. F. Huelga, and M. B. Plenio, Entanglement and Non-Markovianity of Quantum Evolutions, Phys. Rev. Lett. **105**, 050403 (2010).

[19] B. Vacchini, A. Smirne, L. E.-M., J. Piilo, and H.-P. Breuer, Markovianity and non-Markovianity in quantum and classical systems, New J. Phys. **13**, 093004 (2011).

[20] A. Rivas, S. F. Huelga, and M. B. Plenio, Quantum non-Markovianity: Characterization, quantification and detection, Rep. Prog. Phys. **77**, 094001 (2014).

[21] D. Chruscinski and S. Maniscalco, Degree of Non-Markovianity of Quantum Evolution, Phys. Rev. Lett. **112**, 120404 (2014).

[22] I. de Vega and D. Alonso, Dynamics of non-Markovian open quantum systems, Rev. Mod. Phys. **89**, 015001 (2017).

[23] H. Häffner, W. Hänsel, C. F. Roos, J. Benhelm, D. Chek-al kar, M. Chwall, T. Körder, U. D. Rappel, M. Riebe, P. O. Schmidt, C. Becher, O. Gühne, W. Dür, and R. Blatt, Scalable multiparticle entanglement of trapped ions, Nature (London) **438**, 643 (2005).

[24] F. Schwabl, *Advanced Quantum Mechanics* (Springer-Verlag, Berlin, 2008).

[25] M. Walschaers, Signatures of many-particle interference, J. Phys. B: At. Mol. Opt. Phys. **53**, 043001 (2020).

[26] M. Walschaers, Efficient quantum transport, Ph.D. dissertation, Albert-Ludwigs-Universität Freiburg, 2016.

[27] A. Buchleitner, D. Delande, and J.-C. Gay, Microwave ionisation of three-dimensional hydrogen atoms in a realistic numerical experiment, J. Opt. Soc. Am. B **12**, 505 (1995).

[28] Using the identity $\mathbb{1}_{\mathcal{H}_{\rm eff}^N}=\sum_{k=0}^{N}\Pi_k$, with Π_k the projector onto the k-particle subspace, and defining the normalized k-particle states $|\psi_k\rangle=c_k^{-1}\Pi_k|\psi\rangle$, with $c_k=\sqrt{\langle\psi|\,\Pi_k\,|\psi\rangle}$, $c_k\geqslant 0$, we can write $|\psi\rangle=\sum_{k=0}^{N}\Pi_k|\psi\rangle=\sum_{k=0}^{N}c_k|\psi_k\rangle$. For $c_k=0$, the corresponding state $|\psi_k\rangle$ can be chosen arbitrarily.

[29] A. J. Leggett, Bose-Einstein condensation in the alkali gases: Some fundamental concepts, Rev. Mod. Phys. **73**, 307 (2001).

[30] K. Sakmann, A. I. Streltsov, O. E. Alon, and L. S. Cederbaum, Reduced density matrices and coherence of trapped interacting bosons, Phys. Rev. A **78**, 023615 (2008).

[31] M. A. Ruskai, Beyond strong subadditivity? Improved bounds on the contraction of generalized relative entropy, Rev. Math. Phys. **06**, 1147 (1994).

[32] A. Nielsen and B. Chuang, *Quantum Computation and Quantum Information* (Cambridge University Press, Cambridge, 2000).

[33] P. M. Preiss, J. H. Becher, R. Klemt, V. Klinkhamer, A. Bergschneider, N. Defenu, and S. Jochim, High-Contrast Interference of Ultracold Fermions, Phys. Rev. Lett. **122**, 143602 (2019).

[34] V. A. Benderskii and E. I. Kats, Coherent oscillations and incoherent tunneling in a one-dimensional asymmetric double-well potential, Phys. Rev. E **65**, 036217 (2002).

[35] S. Hunn, K. Zimmermann, M. Hiller, and A. Buchleitner, Tunneling decay of two interacting bosons in an asymmetric double-well potential: A spectral approach, Phys. Rev. A **87**, 043626 (2013).

[36] S. Hunn, Microscopic theory of decaying many-particle systems, Ph.D. dissertation, Albert-Ludwigs-Universität Freiburg, 2013.

[37] J. Brugger (unpublished).

[38] S. Bartels, *Numerical Approximation of Partial Differential Equations* (Springer, New York, 2016).

[39] J. Sun and A. Zhou, *Finite Element Methods for Eigenvalue Problems* (CRC Press, Boca Raton, FL, 2017).

[40] C. Dittel, G. Dufour, G. Weihs, and A. Buchleitner, Wave-Particle Duality of Many-Body Quantum States, Phys. Rev. X **11**, 031041 (2021).

[41] J. A. Yeazell and C. R. Stroud Jr., Observation of fractional revivals in the evolution of a Rydberg atomic wave packet, Phys. Rev. A **43**, 5153 (1991).

[42] For these initial states, we have reduced trace distances $D[\hat{\rho}_S^{kp}(0), \hat{\sigma}_S^{kp}(0)] \in \{0, \frac{3}{10}, \frac{3}{5}, \frac{4}{5}, \frac{9}{10}\}$ for $1 \leqslant k \leqslant 5$, and a full trace distance $D(\hat{\rho}_S, \hat{\sigma}_S) = \frac{19}{20}$. The latter value strictly smaller than one in particular shows that the two states under scrutiny here are not entirely orthogonal.

[43] J. B. Conway, *A Course in Operator Theory* (American Mathematical Society, Providence, Rhode Island, 2000).